PHASE-DEPENDENT SITE EFFECTS EMPIRICALLY ESTIMATED

Susumu Kurahashi[1], Kazuaki Masaki[2] and Kojiro Irikura[3]

[1] *Post Doctoral Researcher, Disaster Prevention Research Center, Aichi Institute of Technology. Japan*
[2] *Professor, Dept. of Structural Engineering, Aichi Institute of Technology. Japan*
[3] *Professor, Disaster Prevention Research Center, Aichi Institute of Technology. Japan*
Email:susumu@aitech.ac.jp, masaki@aitech.ac.jp, irikura@geor.or.jp

ABSTRACT :

We developed a method for estimation of site effects in time function using observed records. So far, most of the empirical methods estimate the site effects with only amplitude spectra. Phase characteristics of the site effects have been assumed to be random in simulating strong ground motions. In this study, we attempt to separate the site effects in time domain from observed records. The site effects estimated in the above method are generally different for individual earthquakes. There are coherent site effects commonly included in different records and incoherent ones varying in different records. The coherent site effects are estimated by stacking the site effects in frequency domain synchronizing the onsets of S-waves from individual earthquakes. The incoherent site effects are estimated as power spectra subtracting the power spectra of the coherent site effects from those of the total site effects. The amplitude characteristics of the site effects are estimated as the sum of the amplitude spectra of the coherent ones and square root of the power spectra of the incoherent ones. The phase characteristics of the site effects are given the same as those of the coherent ones. The site effects in time domain are estimated by the inverse Fourier transform of those calculated above in frequency domain. We applied this method to estimating strong ground motions of the 2003 Tokachi-oki earthquake by the stochastic Green's function method including the empirical site effects. We found the synthesized ground motions agreed well with the observed records.

KEYWORDS: empirical site effects, phase-dependent site effects, simulation of ground motion

1. Introduction

Estimation of ground motions of large earthquakes is important for making countermeasures of earthquake disaster mitigation. Failure behavior of structures under large deformation due to strong ground motions has been not always clarified. This means that we have to accumulate ground motion data in disaster areas where collapsed and partially-collapsed structures existed during past disastrous earthquakes. However, it is not so easy to obtain such data. An alternative way is to simulate strong ground motions with time histories in heavily-damaged areas during large earthquakes.

Ground motions during earthquakes are expressed as a convolution of source effects, propagation-path effects and site effects. The site effects are evaluated by theoretical method if we have ground structures beneath the object sites. However, it is very difficult to obtain the information about complex ground structures accurately enough for estimating the site effects in broad-band from 0.1 to 10 Hz of engineering interest. Empirical methods for the site effects are more practical than theoretical ones.

So far, most of the empirical methods estimate site responses with only amplitude spectra (e.g. Iwata and Irikura, 1989; Tsurugi et al., 1997). To obtain the site effects with time histories, phase characteristics were assumed to be random in simulated strong motions. Resultantly, the site effects in time domain become physically meaningless.

On the other hands, Birgören and Irikura (2004) proposed a technique for estimating the site effects with not only amplitude but also phase characteristics using the Meyer-Yamada wavelet procedure (Yamada and Ohkitani, 1991). The site responses at a station directly from its time domain data are estimated by removing source and path effects at each wavelet level, keeping the phase information.

However, the method using the Meyer and Yamada wavelet transform has a weak point that the precision of the

analysis deteriorates in the low frequency range. Therefore, we attempt to estimate the phase-dependent site effects using the Fourier transform procedure The Fourier transform has an advantage that keep the same precision in the all frequency range.
In this paper, we first show the validity of the method we propose using the test data with a signal and noises. The signal corresponds to a true site response which is commonly included in observed data at plural stations from different earthquakes. The noises are included independently in the observed data from different earthquakes, being uncorrelated with each other.
Next, we estimate phase-dependent site effects in the Fourier domain using observed records at stations from aftershocks of the 2003 Tokachi-oki earthquake. The site effects in time domain are obtained by the inverse Fourier transform. Then, we synthesize ground motions from the mainshock using the stochastic Green's function method. The verification and applicability are shown by comparison between the synthesized motions and observed records.

2. Methodology

2.1 Empirical amplitude-spectra site effects

First, we outline the conventional method of empirical amplitude-spectra site effects (e.g. Tsurugi et al., 1997). The observed records $F_{ij}(t)$ from the *i*-th earthquake in time domain are expressed as the convolution of the source, path and site effects in the form Eqn. 1. In frequency domain, these are expressed as the product of those three effects in the form Eqn. 2.

$$F_{ij}(t) = S_i(t) * P_{ij}(t) * G_j(t) \tag{1}$$

$$F_{ij}(f) = S_i(f) P_{ij}(f) G_j(f) \tag{2}$$

where $S_i(t)$ is the source effect of the *i*-th earthquake, $P_{ij}(t)$ is the propagation-path effect from the *i*-th earthquake to the *j*-th station, $G_j(t)$ is the site effect of the *j*-th station. The source effect is assumed the ω^2 model (Brune, 1970) in the form Eqn. 3 following Boore (1983).

$$S_i(f) = Mo_i \frac{R_{\theta\phi} Fs P_{RTITN}}{4\pi\rho Vs^3} \frac{2\pi f}{1+(f/f_{ci})^2} \tag{3}$$

where Mo is seismic moment, $R_{\theta\phi}$ is the radiation pattern, Fs is the amplification due to the free surface, P_{RTITN} is the partitioning of energy into two horizontal components, ρ and Vs are density and S wave velocity of the medium, respectively.
The propagation path effect is given as

$$P_{ij}(f) = \frac{1}{R_{ij}} \exp\left(\frac{-\pi R_{ij} f}{Q(f) Vs}\right) \tag{4}$$

where R_{ij} is the hypocentral distance between the *i*-th event and *j*-th station, $Q(f)$ is the quality factor of frequency dependence.
Therefore, the site effect is calculated as a ratio of the observed records to the multiplication of the source and the propagation-path effects in the form Eqn. 5. The multiplication of the source and the path effect express the spectrum at bed-rock beneath the object station.

$$\left|G_{ij}(f)\right| = \frac{\left|F_{ij}(f)\right|}{S_i(f) P_{ij}(f)} \tag{5}$$

The site effect of the object station is estimated as average of the site effects of individual earthquakes in the form Eqn. 6.

$$G_{jave}(f) = \sqrt[N]{\prod_{i=1}^{N} \left|G_{ij}(f)\right|} \tag{6}$$

2.2 Empirical phase-dependent site effects

We propose a method for empirically estimating phase-dependent site effects. First, the Fourier transforms of

the observed records $F_{ij}(f)$ are made synchronizing the onsets of the S-waves from individual earthquakes. The site effects are estimated with complex Fourier transforms.

$$G_{ij}(f)=\frac{F_{ij}(f)}{S_i(f)P_{ij}(f)} \tag{7}$$

The average should be arithmetically made.

$$G_{jave}(f)=\frac{1}{N}\sum_{i=1}^{N}G_j(f) \tag{8}$$

The site effects estimated in the Form (7) are different for different earthquakes, because generally underground structures near the sites are not flatly-layered. There are coherent site effects commonly included in different records and incoherent ones varying in each record. In this study, we call the coherent site effects signal, and call the incoherent ones noise.

In general, the site effects $g_i(t)$ for the *i*-th earthquake are expressed as the sum of a signal $s(t)$ and noise $n_i(t)$.

$$g_i(t)=s(t)+n_i(t) \tag{9}$$

The signal is commonly included in different records. The noise is independently included in observed records. The purpose of this study is to calculate the site effects commonly included in observed records. There are two approaches to extract the site effects from observed records. One is to take a geometric mean of the site effects changing at every earthquake and the other is to take an arithmetic mean of them. Therefore, we examined the difference between those two approaches.

The site effects $g_i(f)$ from observed records due to the *i*-th earthquake are expressed in frequency domain in the form Eqn. 10. When the common site effect included in different records is estimated by the geometry mean, the amplitude and phase characteristics of the site effect are expressed as the form Eqn. 11 and 12.

$$g_i(f)=A_i(f)\cdot\exp(\phi_i(f)) \tag{10}$$

$$A_{ave}(f)=\sqrt[N]{\prod_{i=1}^{N}A_i(f)} \tag{11}$$

$$\phi_{ave}(f)=\sum_{i=1}^{N}\frac{\phi_i(f)}{N} \tag{12}$$

where N is number of earthquakes.

On the other hands, when the common site effect is estimated by the arithmetic mean, the amplitude and phase characteristic of the site effects are expressed as follows.

$$g_i(f)=\mathrm{Re}(g_i(f))\cdot\cos(f)+l\,\mathrm{Im}(g_i(f))\cdot\sin(f) \tag{13}$$

$$A_{ave}(f)=\sqrt{\frac{1}{N}\sum_{i=1}^{N}\mathrm{Re}(g_i(f))^2+\frac{1}{N}\sum_{i=1}^{N}\mathrm{Im}(g_i(f))^2} \tag{14}$$

$$\phi_{ave}(f)=\arctan\left(\frac{\sum_{i=1}^{N}\frac{\mathrm{Im}(g_i(f))}{N}}{\sum_{i=1}^{N}\frac{\mathrm{Re}(g_i(f))}{N}}\right) \tag{15}$$

where l is imaginary unit and Re is for real part and Im is for imaginary part.

3. Verification of this method

3.1 Test data

In this section, we examine applicability of this method using the test data for the site effects. The test data are given as the sum of a signal and random noise as shown in the left of Figure 1. The data length is 81.92

seconds. The signal is defined as sweep wave from 10 seconds to 70 seconds and zero amplitude in the rest. The Fourier spectra of the signal and the noise are shown in the right of Figure 1. The amplitude spectra of the signal are less than those of the noise from 0.1 to 1.0 Hz, although they are almost the same at frequencies more than 1.0 Hz. We made many test data with the same signal and different noise ramdomly generated. In the top of Figure 2 is shown the signal and in the second to the bottom of Figure 2 are ten of the test data.

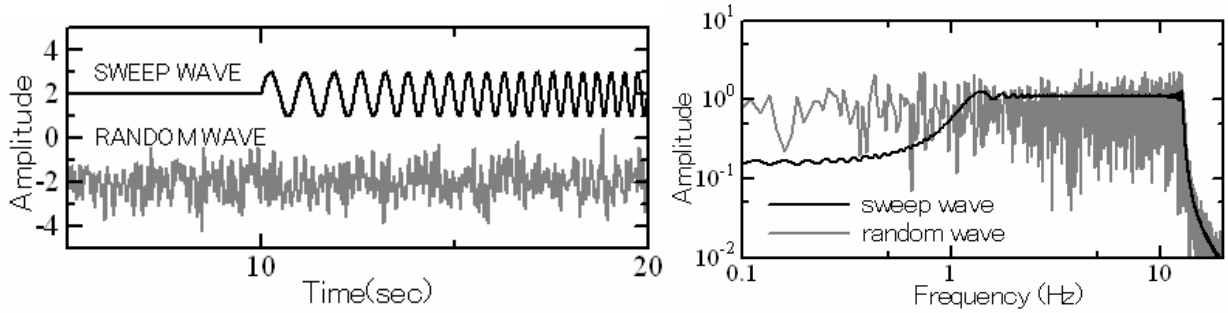

Figure 1 Left: Time histories of a signal (upper) with sweep wave and a noise (lower) with random wave. Right: Fourier spectrum of the signal (upper) and that of the noise (lower).

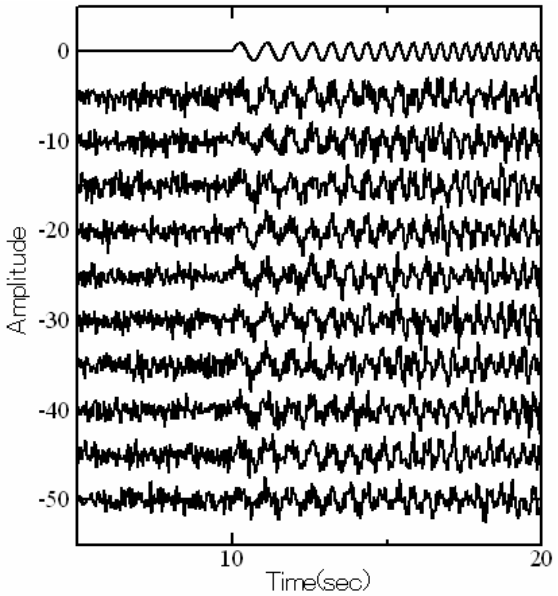

Figure 2 Test data used for analysis. The signal is shown at the top and 10 test data are shown at the second to bottom.

3.2 Verification of the method using test data

We calculate the geometric and arithmetic means of those ten test data shown in Figure 2. As shown in Figure 3, both means have almost the same amplitude spectra as the signal has in the frequency range from 1 Hz to 10 Hz, where the spectrum of the signal is dominant. The arithmetic mean has less amplitude than the geometric mean in the range less than 1 Hz, being closer to the spectral level of the signal in Figure 3.

In the left of Figure 4 are shown the signal, the geometric mean, and the arithmetic mean in time domain. We find that the arithmetic mean has clearly better shape, cancelling out the noises and extracting the signal. However, the geometric mean does not effectively cancel out the noises. The phase characteristics of those two means are compared with those of the signal. To do so, we calculate the group delay time i.e. derivative of the phase spectra with respect to frequency, because it can show the difference of the phase characteristics.

In the right of Figure 4, the group delay time of the arithmetic mean agrees well with that of the signal especially in the frequency range from 1 Hz to 10 Hz, where the amplitude spectra of the signal are dominant. On the other hand, the group delay time of the geometric mean has large deviation from that of the signal, especially in the range less than 3 Hz. These results show that the arithmetic mean is better than the geometric mean to extract the signal from noisy data.

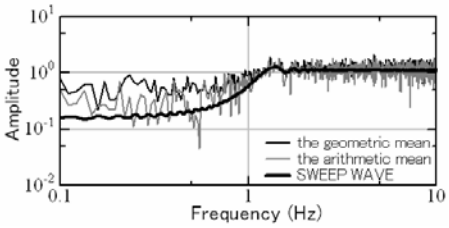

Figure 3 Fourier amplitude spectra of the geometric (black line) and the arithmetic means (gray line) of the test data and the signal with sweep wave (thick line).

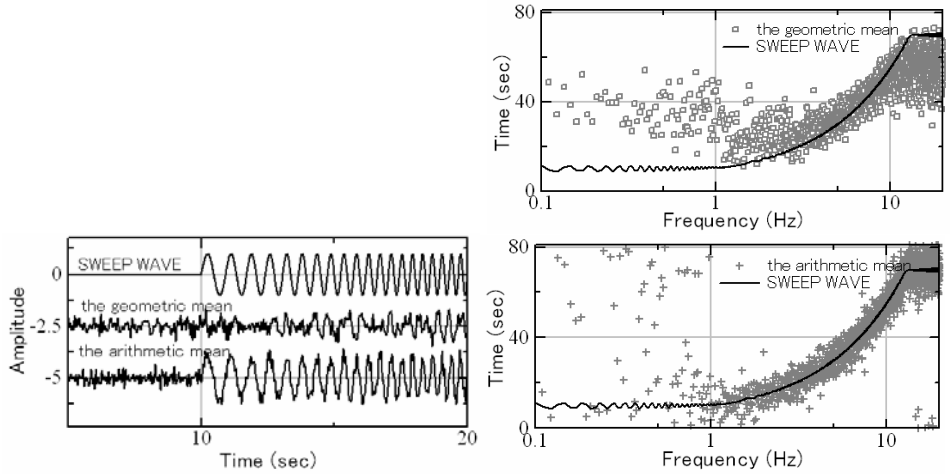

Figure 4 Left: Time histories of the signal (uppermost), the geometric (middle) and arithmetic means (bottom) of the test data. Right upper: Group delay times of the signal (black line) and the geometric mean (small circle). Right lower: Group delay times of the signal (black line) and the arithmetic mean (small cross).

4. Application to simulation of ground motions from the 2003 Tokachi-oki earthquake

After validating the method using test data, we applied it to estimating the site effects in time domain at strong motion stations in the Tokachi region, Hokkaido, Japan. Then, we simulate ground motions from the 2003 Tokachi-oki earthquake, combining the site effects estimated here with the stochastic Green's function method. We use observed records from six earthquakes with the JMA magnitude 4.6 to 5.8, all of which are aftershocks of the 2003 Tokachi-oki earthquake. The epicenters of the earthquakes and the locations of the stations are shown in Figure 5. The data length of the analyzed records is 40.96 seconds.

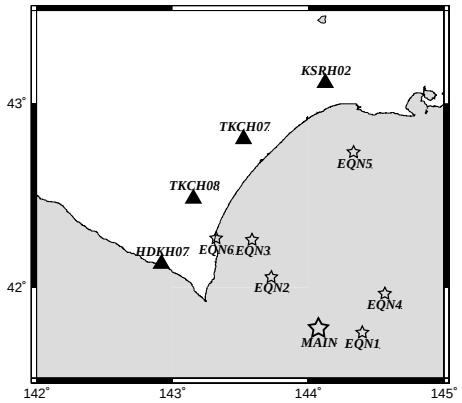

Figure 5 Map showing strong motion stations and epicenters of aftershocks used for analysis

Table 1 Source parameters of aftershocks of the 2003 Tokachu-oki earthquake used for analysis

	date	Mo (Nm)	fc (Hz)	Mj
EQ1	2003/9/26 6:02	1.61E+17	0.60	5.5
EQ2	2003/9/26 7:20	6.24E+16	0.70	5.2
EQ3	2003/9/26 7:24	6.80E+15	1.20	4.6
EQ4	2003/9/26 11:35	5.02E+17*	0.40	5.8
EQ5	2003/9/27 17:06	1.02E+17*	0.60	5.2
EQ6	2003/9/28 9:23	3.95E+16*	0.80	5.0

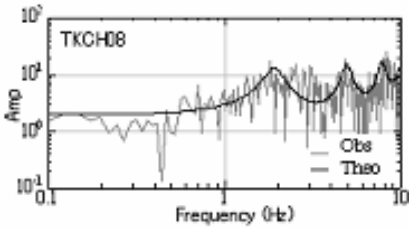

Figure 6 Comparison between a site effect empirically estimated and that theoretically calculated from the ground structure at TKCH08

4.1 Estimation of empirical site effects

First, we calculated the source effects which are needed to estimate the site effects. Most of the seismic moments of earthquakes analyzed here were determined by the F-net of the NIED. However, some were not because the observed data were not enough to do that. The seismic moments of such earthquakes were estimated from the flat-level of displacement spectra at stations. To avoid the amplification due to surface geology we used borehole records at the TKCH08 station which are put in bedrock. The corner frequencies also were read by eye from the displacement spectra to estimate source areas of the earthquakes. Tabe.1 shows the seismic moment and corner frequency of each earthquake.

We also need to have Q-value to estimate the propagation-path effects. We adopted the Q value by Sato and Tatsumi (2002) as follows:

$$Qs(f) = 114 f^{0.92} \qquad f \geq 0.4$$
$$Qs(f) = 114 \qquad f < 0.4 \tag{16}$$

The empirical site effects estimated using the form Eqn. (12) coincide with amplification from seismic bedrock up to surface. We compare the site effects at TKCH08 with those calculated using underground structures beneath the site in Figure 6. Both site effects agree well each other in amplitude levels and dominant frequencies. This result means the validity of seismic moment and corner frequency used here to calculate the site effects.

Next, we calculated the site effects due to arithmetic means of complex Fourier transform.

The coherent site effects are estimated by stacking observed records synchronizing the onsets of S-waves of individual earthquakes. The onsets of S-wave were calculated by the AIC of the AR model which estimate change in the time series. Figure 7 shows the site effects in time domain at TKCH08 estimated from 7 earthquakes.

The shapes of the site effects are remarkably influenced dependent on the hypocentral distances from the earthquakes. For example, the site effects for EQ1 and EQ4 at relatively further distance seem to be dominant at low frequencies. On the other hands, those for EQ2, EQ3, EQ6 at shorter distance are dominant at high frequencies. When the hypocentral distance is large, the propagation-path effects are not simple, then it is very difficult to distinguish between the propagation-path and the site effects. However, our purpose is to get the common effects of observed record from individual earthquakes. Figure.8 shows the site effects in time domain at four stations, HDKN07, KSRH02, TKSH07, and TKCH08. The waveforms of the site effects show site-specific characteristics at every site. For example, the duration of the waveform at TKCH08 is very short, because the ground structure there is hard.

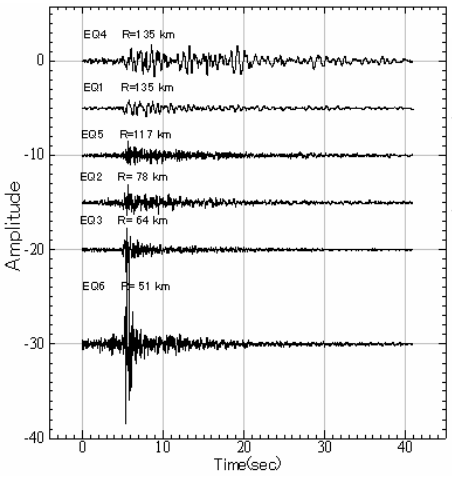

Figure 7 Empirical site effects in time domain at TKCH08 for six earthquakes

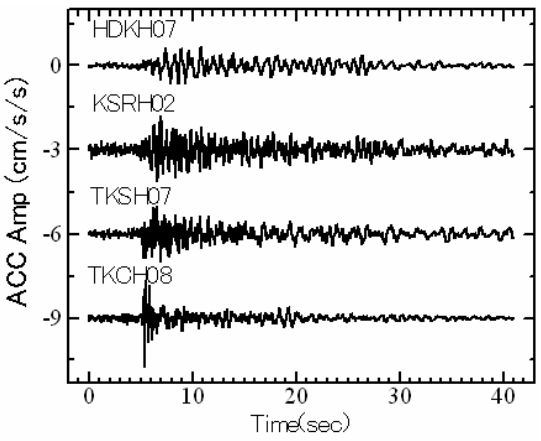

Figure 8 Empirical site effects in time domain at four stations, HDKH07, KSRH02, TKSH07,

4.2 The comparison between synthesized and observed records from the2003 Tokachi-oki earthquake

We simulate ground motions from the 2003 Tokachi-oki earthquake taking into account the empirical site effects. The source model of the 2003 Tokachi-oki earthquake was estimated from the waveform inversions

using teleseismic data and strong motion data by many authors. Almost all of these models are available for low-frequency data less than 1Hz. On the other hands, Kamae and Kawabe estimated the source model using the empirical Green's function method which can estimate available for broad-band. The source model consists of three asperities with stress drop of 25 MPa. The locations of the source fault we used and those three asperities are shown in figure 9.

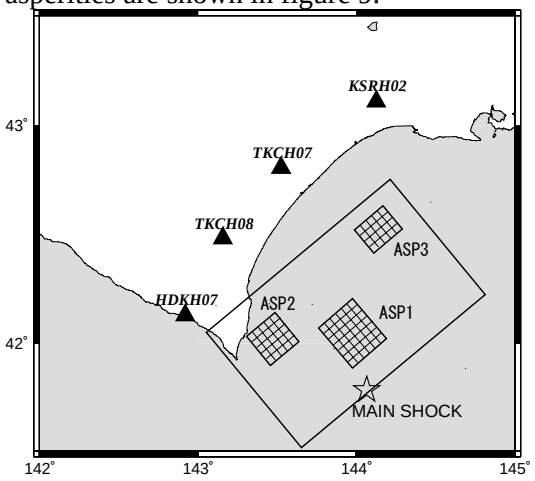

Figure 9 The source model consisting of three asperities estimated by Kamae and Kawabe (2006).

Table 2 Parameters of three asperities of the 2003 Tokachi-oki earthquake used for analysis

	Mo (Nm)	L(km)×W(km)	⊿σ (MPa)
ASP-1	1.99E+21	24×28	25
ASP-2	8.75E+19	20×20	25
ASP-3	6.43E+19	20×16	25

Table 3 Source parameters of a small event used as the empirical Green's function

	Mo (Nm)	Fc(Hz)	S(km^2)	⊿σ (MPa)
EGF	1.40E+17	0.7	16	5

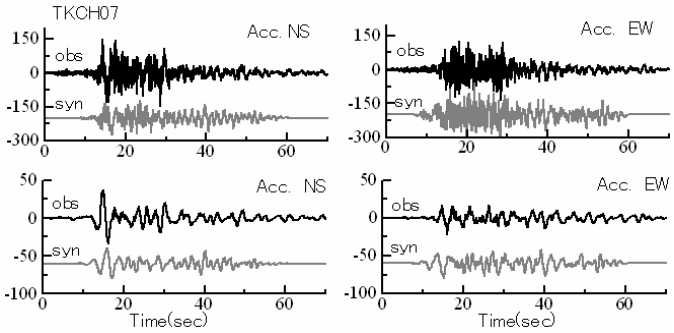

Figure 10 Comparison between synthesized motions (gray line) and observed record (black line) at TKCH07 from the 2003 Tokachi-oki earthquake.

When we use the stochastic Green's function method, we need to have source effects of small events, propagation-path and site effects. The source effects and the propagation-path were derived from Form Eqn. 3 and 4, respectively. Then, the seismic moment and fault area of the small events were assumed to be 1.4E+17Nm and 16km2, respectively, as shown in Table 3.

In this study, we calculated ground motions generated only from three asperities, ASP1, ASP2, and ASP3. Comparison between the synthesized ground motions (gray line) and observed records (black line) at TKCH07 were shown in Figure 10. We consider that the duration and pulse of the synthesized acceleration and velocity waveforms were similar to those of observed ones, although the amplitude was a little underestimated.

The site effects used here for simulation were the coherent ones. The incoherent ones were cancelled out by stacking when the site effects are calculated. This might be a reason why the synthesized motions were underestimated. Therefore, we recalculated the site effects. The amplitude characteristics of the site effects are estimated as the sum of the amplitude spectra of the coherent ones and square root of the power spectra of the incoherent ones. The phase characteristics of the site effects are assumed to be the same as those of the coherent ones.

The synthesized motions recalculated using the site effects mentioned above were compared with the observed records in Figure 11. The synthesized motions at TKCH07 and HDKH07 fit better to the observed ones. Especially, pulse of S wave of synthesized at TKCH07 is agree well with observed ones.

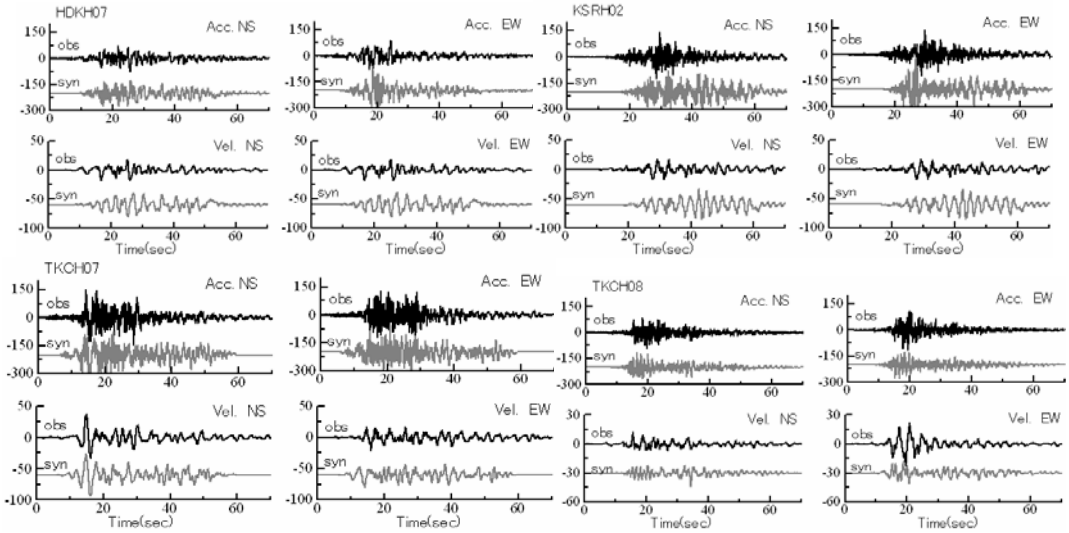

Figure 11 Comparison between the synthesized motions (gray line) and observed records (black line) from the 2003 Tokachi-oki earthquake

5. CONCLUSION

We have proposed a method for estimating phase-dependent site effects to simulate ground motions from future large earthquakes. Validity of the method have been clarified applying it to test data with a signal and noise and observed records from actual earthquakes.

1) We need to calculate empirical site effects by the arithmetic means to keep the phase characteristics correctly. The geometric means distort the phase characteristics included in the observed records.

2) The site effects for simulation should be defined to be coherent and incoherent site effects. Synthesized motions using only coherent site effects are underestimated compared with observed records.

3) Ground motions from the 2003 Tokachi-oki earthquake are well simulated using the empirical site effects and the stochastic Green's function method.

ACKOWLEDFMENTS

We used the wave data provided by the Kik-net of National Research Institute for Earth Science and Disaster Prevention (NIED). We also used the hypocentral information from JMA, and the moment tensor solution from the F-net (NIED). Some figures were made using the GMT plotting package (Wessel and Smith, 1998)

REFERENCES

Birgören, G. and Irikura, K. (2004), Estimation of site response in time domain using the Meyer-Yamada wavelet analysis, Bull. Seism. Soc. Am., 73, 1865-1894.

Boore, D.M. (1983), Stochastic simulation of high-frequency ground motion based on seismological models of the radiated spectra, Bull. Seism. Soc. Am., 74, 1969-1993.

Brune, J.N. (1970), Tectonic stress and the spectra of seismic shear waves from earthquakes, J. Geophys. Res. 75, 4997-5009.

Iwata, T. and Irikura, K. (1986), Separation of Source, Propagation and Site Effects from Observed S-Waves, Zishin (J. Seism.Soc.Jpn.), 39, 579-593.

Kamae, K. and Hidenori, K. (2006), Source modeling of recent large subduction earthquakes in Japan, ESG2006, Grenoble.

Sato, T. and Tatsumi, Y. (2002), Source, path, and site effects for crustal and subduction earthquake inferred from strong motion records in Japan, J. Struct. Constr. Eng., AIJ, 556, 15-24.

Tsurugi, M., Tai, M., Irikura, K. and Kowada, A. (1997), Estimation of Empirical Site Amplification Effects Using Observed Records, Zishin(J. Seism.Soc.Jpn.), 50, 215-227.

Yamada, M. and Ohkitani, K. (1991), Orthonormal wavelet analysis of turbulence, Fluid Dyn. Res. 8, 101-115.